International Journal of Innovative
Computing, Information and Control
Volume **16**, Number **1**, February **2020**

 ISSN 1349-4198
pp. **189–205**

# APPLICATION OF CUCKOO SEARCH TO ROBUST PIDA CONTROLLER DESIGN FOR LIQUID-LEVEL SYSTEM

Thiwa Jitwang and Deacha Puangdownreong

Department of Electrical Engineering
Southeast Asia University
19/1 Petchkasem Road, Nongkhangphlu, Nonghkaem, Bangkok 10160, Thailand
deachap@sau.ac.th

Received February 2019; revised August 2019

Abstract. *The cuckoo search (CS) is one of the most efficient nature-inspired metaheuristic algorithms for solving optimization problems. In this paper, the application of the CS to optimally design robust proportional-integral-derivative-accelerated (PIDA) controller for the three-tank (3-tank) liquid-level control system is presented. Such the 3-tank liquid-level control system commonly exists in industries under the proportional-integral-derivative (PID) control loop. However, the PIDA could provide better responses than the PID for higher order plant. Based on the modern optimization context, designing the robust PIDA controller for the 3-tank liquid-level control system with model uncertainty can be formulated by using the CS as an optimizer. The CS-based robust PIDA controller design framework can be considered as the constrained optimization problem. Model uncertainty occurs due to aging and environmental effects. Results obtained by the robust PIDA controller designed by the CS are compared with those obtained by the PID controller designed by Ziegler-Nichols (ZN) tuning rule and the CS, respectively. As simulation results, it was found that the responses of the 3-tank liquid-level controlled system with the robust PIDA controller designed by the CS are superior to those with the PID controller designed by ZN and CS. In addition, due to model uncertainty within* $\pm 10\%$ *of each lumped parameter of the nominal plant model, the robust PIDA controller designed by the CS could provide the satisfactory responses corresponding to inequality constraint functions. The robust performance and robust stability of the 3-tank liquid-level controlled system are elaborately assured.*

**Keywords:** Robust PIDA controller, Cuckoo search, Model uncertainty, Three-tank liquid-level system

1. **Introduction.** Most real-world design optimization problems in engineering are often highly complex and their optimal solutions cannot be provided by conventional optimization techniques. Based on the modern optimization context, metaheuristic algorithms have been more and more accepted for solving real-world design optimization problems [1,2]. The cuckoo search (CS), one of the most efficient nature-inspired metaheuristic algorithms, was firstly proposed by Yang and Deb in 2009 [3] to solve the combinatorial optimization problems. The CS algorithm is based on the obligate brood parasitic behavior of some cuckoo species in combination with the Lévy flight behavior of some birds and fruit flies. Following the literature, the CS algorithm was proved for the global convergent property [4]. Moreover, it was successfully applied to many real-world engineering problems, such as wind turbine blades [5], antenna arrays [6], power systems [7], travelling salesman problem [8], structural optimization problem [9], wireless sensor network [10], flow shop scheduling problem [11], job shop scheduling problem [12], model order

DOI: 10.24507/ijicic.16.01.189

reduction [13] and control systems [14]. The state-of-the-art and various applications of the CS have been reviewed and reported [15].

In many industrial applications, the liquid-level control in tanks containing different chemicals or mixtures is very important, for example, filtration, dairy, effluent treatment, waste water treatment plant, food processing, nuclear power generation plants, pharmaceutical industries, water purification systems, industrial chemical processing and spray coating as well as boilers [16]. Liquid-level control is commonly large lag, time varying and complex system. The main objective of such the control systems is to fill the tank as quickly and smoothly as possible. The three-tank (3-tank) system relates to liquid-level control generally existing in industrial surge tanks. The 3-tank liquid-level control is classified as process control. It can be considered as non-interaction and interaction. However, the later one is more complicate than the former one. By literature reviews, it was found that in process control applications more than 95% of the controllers are the proportional-integral-derivative (PID) controllers [17]. Well-known tuning design methods for designing the PID controller of process control are Ziegler-Nichols (ZN), Chien, Hrones and Reswick (CHR) and Cohen-Coon (CC) tuning rules [17].

In 1996, the proportional-integral-derivative-accelerated (PIDA) controller was firstly proposed by Jung and Dorf [18]. The PIDA controller, possessing three arbitrary zeros and one pole at origin, can provide faster and smoother responses for the higher-order plants than the PID controller. In addition, modern optimization techniques called "metaheuristics" have been widely applied to design the PIDA controller, for instance, the PIDA controller designed by the genetic algorithm (GA) [19], particle swarm optimization (PSO) [20], current search (CuR) [21], firefly algorithm (FA) [22], bat algorithm (BA) [23,24] and flower pollination algorithm (FPA) [25,26].

The applications of the CS to design an optimal PIDA controller for non-interaction 3-tank liquid-level control system do not appear in literature. Until the beginning of 2018, the CS was firstly conducted to design an optimal PIDA controller for non-interaction 3-tank liquid-level control system [27]. Because of its high performance, convergent property and ease to use, the application of the CS to optimally design the robust PIDA controller for the interaction 3-tank liquid-level control system is proposed in this paper. Results obtained by the robust PIDA controller designed by the CS will be compared with those obtained by the PID controller designed by ZN and the CS, respectively. This paper consists of six sections. After an introduction presented in Section 1, the CS algorithm is reviewed in Section 2. Concepts of robust control system consisting of model uncertainty, robust performance and robust stability are described in Section 3. Problem formulation consisting of CS-based robust PIDA controller design optimization framework for the interaction 3-tank liquid-level control system is given in Section 4. Results and discussions are illustrated in Section 5, while conclusions are followed in Section 6.

2. **Cuckoo Search Algorithm.** In 2009, the cuckoo search (CS) was firstly launched by Yang and Deb as one of the most efficient nature-inspired metaheuristic algorithms. The CS algorithm mimics the obligate brood parasitic behavior of some cuckoo species in combination with the Lévy flight behavior of some birds and fruit flies. In the CS algorithm, each cuckoo lays one egg at a time, and dumps it in a randomly chosen nest. The best nests with high quality of eggs (solutions) will carry over to the next generation. The number of available host nests is fixed, and a host can discover an alien egg with a probability $p_a \in [0, 1]$. In this case, the host bird can either throw the egg away or abandon the nest, and build a completely new nest in a new location.

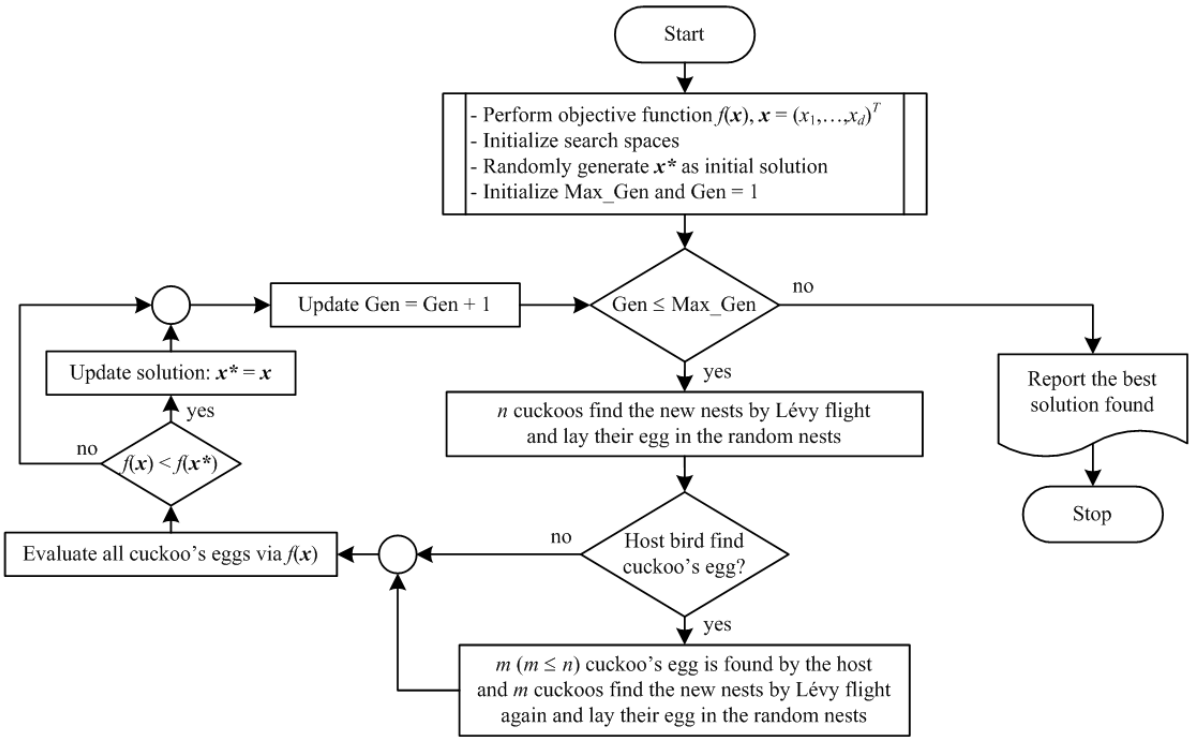


FIGURE 1. Flow diagram of CS algorithm

Objective function $f(\boldsymbol{x})$, $\boldsymbol{x} = (x_1,\ldots,x_d)^T$
Generate initial population of cuckoos $n$ and solution $\boldsymbol{x}_i = (i = 1, 2,\ldots, n)$
Initialize Max_Gen, Gen = 1 and search spaces
**while** (Gen < Max_Gen) or (Termination criterion)
- Get a cuckoo randomly by Lévy flights
- Evaluate its quality via $f(\boldsymbol{x}_i)$
- Choose a nest among $n$ (say, $j$) randomly
**if** $\{f(\boldsymbol{x}_i) < f(\boldsymbol{x}_j)\}$,
- Replace $j$ by the new solution
**end if**
- A fraction ($p_a$) of worse nests are abandoned and new ones are built.
- Keep the best solutions (or nests with quality solutions)
- Rank the solutions and find the current best
- Update Gen = Gen + 1
**end while**
Postprocess results and visualization

FIGURE 2. Pseudo code of CS algorithm

The CS algorithm can be represented by the flow diagram and the pseudo code as visualized in Figure 1 and Figure 2, where $n$ is numbers of cuckoos and $m$ is numbers of cuckoo's eggs that were found by the host bird.

Referring to Figure 1 and Figure 2 representing the CS algorithm, the objective function $f(\boldsymbol{x})$, numbers of population of cuckoos $n$, solutions $\boldsymbol{x}_n$ and a fraction $p_a$ of worse nests are firstly initialized. In the iteration process, the CS algorithm will check the termination criteria (TC), the difference between Gen and Max_Gen, where Gen is a counter and

Max_Gen is the maximum generation preset for terminating the search process. If Gen < Max_Gen, the search process will continue. Otherwise the search process will be stopped. In each iteration, $n$ cuckoos will find the new nests by Lévy flight and lay their eggs in the random nests to create new solutions. After cuckoos lay their eggs, the host bird will check their nests with a fraction $p_a$. If the host bird discovers $m$ ($m \leq n$) alien (cuckoo) eggs that are not its own, it will either throw these $m$ eggs away or simply abandon its nest and build a new nest elsewhere. This means that $m$ cuckoo need to find the new nests by Lévy flight again and lay their eggs in the new random nests to create new solutions. After that, all cuckoo's eggs (new solutions) will be evaluated by the objective function $f(\boldsymbol{x})$ and the current best solution will be updated by new solution found. The CS algorithm will be iteratively processed until the optimal solution is found or the TC are met.

New solutions $\boldsymbol{x}^{(t+1)}$ for cuckoo $i$ can be generated by using a Lévy flight as stated in (1). Symbol Lévy($\lambda$) in (1) represents a Lévy distribution providing random walk with random step drawn from a Lévy distribution having an infinite variance with an infinite mean as expressed in (2). In another way, the step length $s$ of cuckoo flight can be calculated by (3), where $u$ and $v$ are drawn from normal distribution as stated in (4). Standard deviations of $u$ and $v$ are also expressed in (5), where $\Gamma$ is the standard Gamma function.

$$\boldsymbol{x}_i^{(t+1)} = \boldsymbol{x}_i^{(t)} + \alpha \oplus \text{Lévy}(\lambda) \tag{1}$$

$$\text{Lévy} \approx u = t^{-\lambda}, \quad (1 < \lambda \leq 3) \tag{2}$$

$$s = \frac{u}{|v|^{1/\beta}} \tag{3}$$

$$u \approx N\left(0, \sigma_u^2\right), \quad v \approx N\left(0, \sigma_v^2\right) \tag{4}$$

$$\sigma_u = \sqrt[\beta]{\frac{\Gamma(1+\beta)\sin(\pi\beta/2)}{\Gamma[(1+\beta)/2]\beta 2^{(\beta-1)/2}}}, \quad \sigma_v = 1 \tag{5}$$

3. **Robust Control System.** In control system design process, the mathematical model of the plant or controlled system needs to be firstly obtained. In fact, any plant model will include an error from approximation of some elements in the modeling process. In addition, effects of aging and working environment can make the model error. Therefore, the actual plant will differ from the model used in design process. In order to ensure the controller designed based on such the model will work satisfactorily when this controller is used for the actual plant, one reasonable approach is to assume from the beginning that there is an uncertainty or error between the actual plant and its mathematical model and include such uncertainty or error in the design process of the control system. The control system designed based on this approach is called a robust control system which has been developed since around 1980 [28-32].

Let the actual plant be $\tilde{G}_p(s)$ and the mathematical model of the actual plant be $G_p(s)$, that is,

$$\tilde{G}_p(s) = \text{actual plant model having uncertainty } \Delta(s) \tag{6}$$

$$G_p(s) = \text{nominal plant model used for design} \tag{7}$$

$\tilde{G}_p(s)$ and $G_p(s)$ may be related by a multiplicative factor as stated in (8) or an additive factor as expressed in (9).

$$\tilde{G}_p(s) = G_p(s)[1 + \Delta(s)] \tag{8}$$

$$\tilde{G}_p(s) = G_p(s) + \Delta(s) \tag{9}$$

Since the exact description of the uncertainty or error $\Delta(s)$ is unknown, an estimate, $W(s)$, which is estimation term of $\Delta(s)$ is used in the design of the controller. $W(s)$ is a scalar transfer function as stated in (10), where $||W(s)||_\infty$ is the maximum value of $|W(j\omega)|$ for $0 \leq \omega \leq \infty$. $||W(s)||_\infty$ is thus called the $H_\infty$ norm of $W(s)$.

$$||\Delta(s)||_\infty < ||W(s)||_\infty = \max_{0\leq\omega\leq\infty} |W(j\omega)| \tag{10}$$

Regarding to the small-gain theorem, consider the closed-loop system shown in Figure 3, where $\Delta(s)$ and $M(s)$ are stable and proper transfer functions.

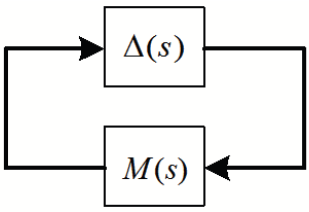


FIGURE 3. Closed-loop system

The small-gain theorem states that if the $H_\infty$ norm of $\Delta(s)M(s)$ stated in (11) is satisfied, then this closed-loop system is stable.

$$||\Delta(s)M(s)||_\infty < 1 \tag{11}$$

That is, if the $H_\infty$ norm of $\Delta(s)M(s)$ is smaller than 1, this closed-loop system is stable. This theorem is an extension of the Nyquist stability criterion. It is important to note that the small-gain theorem gives a sufficient condition for stability. That is, a system may be stable even if it does not satisfy this theorem. However, if a system satisfies the small-gain theorem, it is always stable [28-30].

According to the small gain theorem, the design procedure is to the determination of the controller $G_c(s)$ making the inequality in (12) satisfied, where $G_p(s)$ is the transfer function of the model used in the design process, $G_c(s)$ is the transfer function of the controller and $W(s)$ is the chosen transfer function to approximate $\Delta(s)$.

$$\left\| \frac{W(s)}{1 + G_c(s)G_p(s)} \right\|_\infty < 1 \tag{12}$$

Robust stability means that the controller $G_c(s)$ guarantees internal stability of all systems that belong to a group of systems that include the system with the actual plant, whereas robust performance means the specified performance is satisfied in all systems that belong to the group. To guarantee robust stability and robust performance, two inequalities expressed in (13) and (14) need to be satisfied, where $W_1(s)$ is stable weighting function matrix and $W_2(s)$ is performance weighting function matrix. Both $W_1(s)$ and $W_2(s)$ can be specified by the designers.

$$\left\| \frac{W_1(s)G_c(s)G_p(s)}{1 + G_c(s)G_p(s)} \right\|_\infty < 1, \text{ for robust stability} \tag{13}$$

$$\left\| \frac{W_2(s)}{1 + G_c(s)G_p(s)} \right\|_\infty < 1, \text{ for robust performance} \tag{14}$$

Once setting sensitivity function $S(s)$ and complementary sensitivity function $T(s) = 1 - S(s)$ as stated in (15) and (16), robust stability and robust performance in (13) and (14) can be rewritten as expressed in (17) and (18), respectively.

$$S(s) = \frac{1}{1 + G_c(s)G_p(s)} \tag{15}$$

$$T(s) = 1 - \left(\frac{1}{1 + G_c(s)G_p(s)}\right) = \frac{G_c(s)G_p(s)}{1 + G_c(s)G_p(s)} \tag{16}$$

$$\|W_1(s)T(s)\|_\infty < 1, \text{ for robust stability} \tag{17}$$

$$\|W_2(s)S(s)\|_\infty < 1, \text{ for robust performance} \tag{18}$$

The robust stability and robust performance will be used as the inequality constraints of the robust PIDA controller design approach by the CS as detailed in next section.

4. **CS-Based Robust PIDA Controller Design.** This section proposes the problem formulation of the CS-based robust PIDA controller design optimization for the interaction 3-tank liquid-level system. In this section, the PIDA control loop, the mathematical model of the interaction 3-tank liquid-level system and the CS-based robust PIDA controller design optimization framework are consecutively proposed.

4.1. **PIDA control loop.** The feedback PIDA control loop is represented by the block diagram as shown in Figure 4, where $G_p(s)$ is the 3-tank system model and $G_c(s)$ is the PIDA controller. The PIDA controller receives the error signal $E(s)$ and produces the control signal $U(s)$ to control the output response $C(s)$ and regulate the external disturbance signal $D(s)$ referring to the reference input $R(s)$. The $s$-domain transfer function of the PIDA controller is stated in (19), where $K_p$ is proportional gain, $K_i$ is integral gain, $K_d$ is derivative gain and $K_a$ is accelerated gain. In (19), $a$, $b$, $c$ and $d$, $e$ are zeros and poles of the PIDA controller, respectively. Since $a$, $b$, $c << d$, $e$, the poles $d$, $e$ can be neglected [18]. Therefore, the PIDA transfer function in (19) can be rewritten as expressed in (20). Referring to (20), it can be observed that the PIDA controller possesses three arbitrary zeros and one pole at origin.

$$\left.\begin{aligned} G_c(s)|_{PIDA} &= K_p + \frac{K_i}{s} + \frac{K_d s}{(s+d)} + \frac{K_a s^2}{(s+d)(s+e)} \\ &= \frac{K(s+a)(s+b)(s+c)}{s(s+d)(s+e)} \end{aligned}\right\} \tag{19}$$

$$G_c(s)|_{PIDA} = K_p + \frac{K_i}{s} + K_d s + K_a s^2 \tag{20}$$

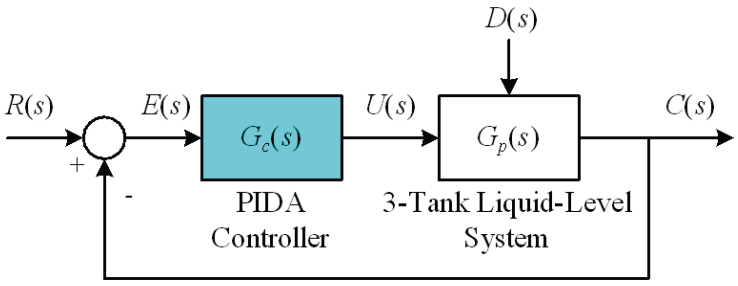


FIGURE 4. PIDA feedback control loop

4.2. **Model of interaction liquid-level system.** According to the magnitude of the Reynolds number, systems involving fluid flow can be divided into laminar and turbulent forms [33]. If the Reynolds number ($R_N$) is less than about 2,000, the flow is laminar. If the $R_N$ is in interval about 2,000 to 4,000, the flow is transition state. Finally, if the $R_N$ is greater than about 4,000, the flow is turbulent as shown in Figure 5, where $x$ is horizontal displacement, $y$ is vertical displacement and $u$ is fluid flow speed.

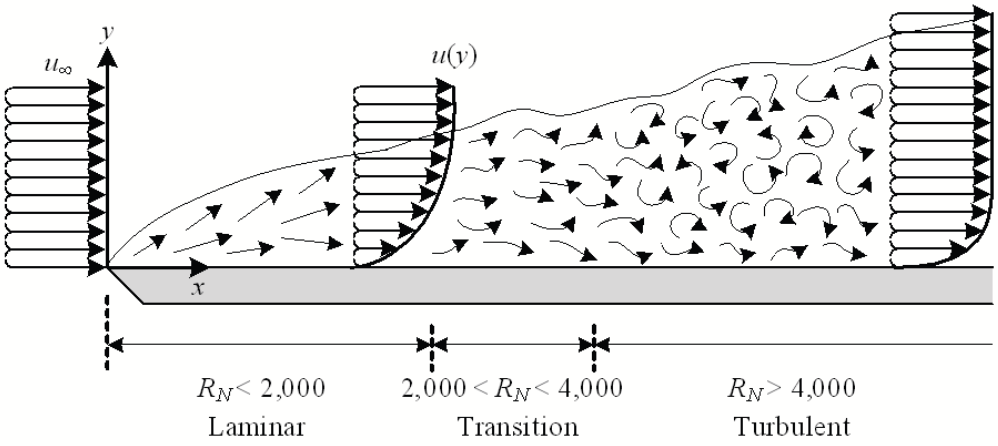


FIGURE 5. Laminar and turbulent flows [33]

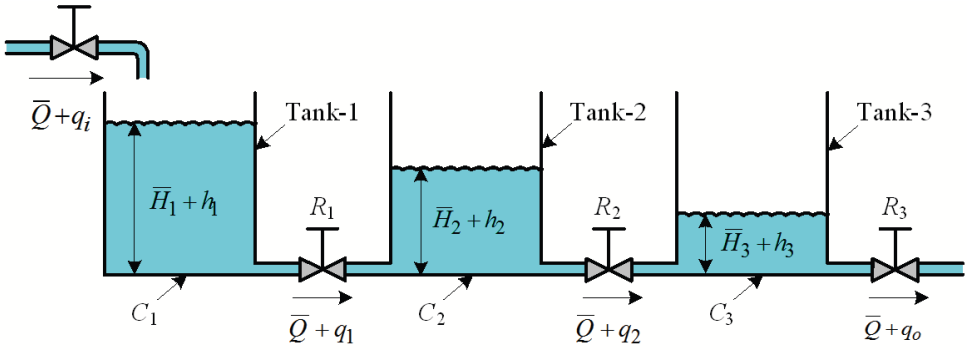


FIGURE 6. Schematic diagram of interaction 3-tank liquid-level system

The schematic diagram of an interaction 3-tank liquid-level system consisting of three first-order processes connected in series can be represented in Figure 6, where

$\bar{Q}$ is steady-state flow rate,
$\bar{H}_j$ is steady-state liquid level of Tank-$j$, where $j = 1, 2, 3$,
$R_j$ is valve resistance of Tank-$j$,
$C_j$ is capacitance (or cross-sectional area) of Tank-$j$,
$h_j(t)$ is liquid level of Tank-$j$,
$q_i(t)$ is liquid inflow rate into Tank-1,
$q_k(t)$ is liquid inflow rate into Tank-$k$, where $k = 1, 2$, and
$q_o(t)$ is liquid outflow rate from Tank-3.

In this work, the linearized mathematical model of an interaction 3-tank liquid-level system is formulated by setting $q_i(t)$ as input variable and $q_o(t)$ as output variable, respectively. Referring to Figure 6, linear differential equations of Tank-1, Tank-2 and Tank-3 are performed as stated in (21)-(23), respectively. The transfer function of an interaction 3-tank liquid-level system is then formulated in (24).

$$\left.\begin{aligned} q_i(t) - q_1(t) &= C_1 \frac{dh_1(t)}{dt} \\ q_1(t) &= \frac{h_1(t) - h_2(t)}{R_1} \end{aligned}\right\} \tag{21}$$

$$\left.\begin{aligned} q_1(t) - q_2(t) &= C_2 \frac{dh_2(t)}{dt} \\ q_2(t) &= \frac{h_2(t) - h_3(t)}{R_2} \end{aligned}\right\} \tag{22}$$

$$\left.\begin{aligned} q_2(t) - q_o(t) &= C_3 \frac{dh_3(t)}{dt} \\ q_o(t) &= \frac{h_3(t)}{R_3} \end{aligned}\right\} \tag{23}$$

$$G_p(s) = \frac{Q_o(s)}{Q_i(s)} = \frac{1}{a_2 s^3 + a_1 s^2 + a_0 s + 1} \tag{24}$$

where $a_0 = R_1C_1 + R_2C_2 + R_3C_3 + R_2C_1 + R_3C_2 + R_3C_1$, $a_1 = R_1R_2C_1C_2 + R_1R_3C_1C_2 + R_1R_3C_1C_3 + R_2R_3C_1C_3 + R_2R_3C_2C_3$ and $a_2 = R_1R_2R_3C_1C_2C_3$.

4.3. **Robust PIDA controller design framework.** Regarding to modern optimization framework, application of the CS to design the robust PIDA controller for an interaction 3-tank liquid-level system can be represented by the block diagram in Figure 7. The objective function $f$ is set as the sum-squared error between the referent inflow rate $R(s)$ and the actual outflow rate $C(s)$ as stated in (25). In order to be minimized, $f$ will be fed to the CS by searching for the appropriate values of the PIDA parameters, i.e., $K_p$, $K_i$, $K_d$ and $K_a$ subject to inequality constraint functions set by the desired response specifications as stated in (26).

$$\text{Min } f(K_p, K_i, K_d, K_a) = \sum_{i=1}^{N} [r_i - c_i]^2 \tag{25}$$

$$\text{Subject to } g_j(K_p, K_i, K_d, K_a) \le 0, \quad j = 1, 2, \ldots \tag{26}$$

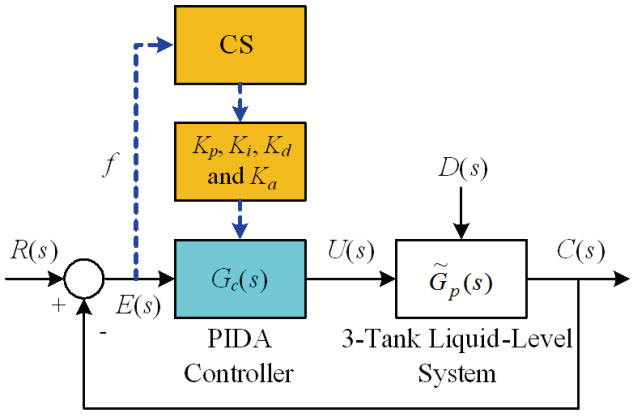


FIGURE 7. CS-based robust PIDA design framework

Referring to (24), the $G_p(s)$ is considered as the nominal plant model. However, with aging and environmental effects, the nominal plant model can be varied. This is called model uncertainty. Based on the robust control theory [28-30], the additive uncertainty term $\Delta(s)$ may be added into $G_p(s)$ as stated in (27). The plant model $\tilde{G}_p(s)$ in (27) will be used as the plant in Figure 7.

$$\left.\begin{aligned} \tilde{G}_p(s) &= G_p(s) + \Delta(s) \\ &= \frac{1}{(a_2 + \Delta)s^3 + (a_1 + \Delta)s^2 + (a_0 + \Delta)s + 1} \end{aligned}\right\} \tag{27}$$

5. **Results and Discussions.** The parameters of the nominal plant model $G_p(s)$ in (24) are set as $R_1 = R_2 = 1.0$ m/m$^3$/sec., $R_3 = 0.5$ m/m$^3$/sec., $C_1 = C_2 = C_3 = 1.0$ m$^2$ [34]. The nominal plant model $G_p(s)$ in (24) can be rewritten as given in (28). For comparison, the PID controller $G_c(s)$ stated in (29) designed by the ZN tuning rule for an interaction 3-tank liquid-level system is firstly presented.

$$G_p(s) = \frac{1}{0.5s^3 + 3s^2 + 4.5s + 1} \tag{28}$$

$$G_c(s)|_{PID} = K_p + \frac{K_i}{s} + K_d s = K_c \left(1 + \frac{1}{\tau_i s} + \tau_d s\right) \tag{29}$$

5.1. **PID controller designed by ZN.** For the second method of ZN tuning rule [35,36], $\tau_i = \infty$ and $\tau_d = 0$ will be firstly set for the PID controller $G_c(s)$ in (29). That is, $G_c(s) = K_c$. The closed-loop transfer function of $G_p(s)$ in (28) and $G_c(s) = K_c$ is shown in (30). The critical gain $K_{cr}$ is the $K_c$ at which the closed-loop system response first exhibits sustained oscillation. The corresponding period $P_{cr}$ can be obtained by the sustained oscillation of the closed-loop system response caused by $K_{cr}$.

$$\frac{C(s)}{R(s)} = \frac{K_c}{0.5s^3 + 3s^2 + 4.5s + 1 + K_c} \tag{30}$$

$K_{cr}$ and $P_{cr}$ can be obtained by the characteristic equation in (31). By substituting $s = j\omega$ in (31), two consecutive equations are performed in (32) and (33).

$$0.5s^3 + 3s^2 + 4.5s + 1 + K_c = 0 \tag{31}$$

$$K_c + 1 - 3\omega^2 = 0 \tag{32}$$

$$\omega\left(4.5 - 0.5\omega^2\right) = 0 \tag{33}$$

From (32) and (33), it was found that $K_{cr} = 26$ and $P_{cr} = 2.0944$ sec. The PID parameters can be calculated from Table 1: $K_c = 0.6K_{cr} = 15.60$, $\tau_i = 0.5P_{cr} = 1.05$ sec. and $\tau_d = 0.125P_{cr} = 0.26$ sec. Therefore, the PID controller designed by the ZN tuning rule for an interaction 3-tank liquid-level system is stated in (34).

$$G_c(s)|_{PID\_ZN} = 15.60 + \frac{14.90}{s} + 4.08s \tag{34}$$

TABLE 1. ZN tuning rule based on ultimate gain $K_{cr}$ and ultimate period $P_{cr}$

| Controllers | Parameters | | |
|---|---|---|---|
| | $K_c$ | $\tau_i$ | $\tau_d$ |
| P | $0.5K_{cr}$ | $\infty$ | 0 |
| PI | $0.45K_{cr}$ | $P_{cr}/1.2$ | 0 |
| PID | $0.6K_{cr}$ | $0.5P_{cr}$ | $0.125P_{cr}$ |

5.2. **PID controller designed by CS.** Regarding to the CS-based robust PIDA design framework in Figure 7, the PID controller designed by the CS for the interaction 3-tank liquid-level system can be performed. The objective function $f$ in (25) is modified as stated in (35) to be minimized by the CS subjecting to inequality constraint functions defined from desired response specifications as expressed in (36).

The CS algorithm was coded by MATLAB version 2018b (License No.#40637337) run on Intel(R) Core(TM) i5-3470 CPU@3.60 GHz, 4.0 GB-RAM. The searching parameters of CS are set according to the recommendations of Yang and Deb [3,4] as follows: number of cuckoos $n = 40$ and fraction $p_a = 0.2$. This searching parameters setting is sufficient for

most optimization problems because the CS algorithm is very robust (not very sensitive to the parameter adjustment) [3,4]. Search spaces and constraint functions are then performed as shown in (36), where $t_r$ is rise time, $M_p$ is the percent maximum overshoot, $t_s$ is the settling time and $E_{ss}$ is the steady-state error, respectively. The maximum generation Max_Gen = 100 is then set as the termination criteria (TC). 50 trials are conducted to find the best solution (optimal PID controller for the interaction 3-tank liquid-level system). When the search process stopped, the CS can successfully provide the optimal parameters of the PID controller of the interaction 3-tank liquid-level system as expressed in (37).

$$\text{Min } f(K_p, K_i, K_d) = \sum_{i=1}^{N} [r_i - c_i]^2 \tag{35}$$

$$\left.\begin{array}{ll} \text{Subject to} & t_r \le 2.5 \text{ sec.}, \\ & M_p \le 20.0\%, \\ & t_s \le 15.0 \text{ sec.}, \\ & E_{ss} \le 0.01\%, \\ & 0 < K_p \le 30, \\ & 0 < K_i \le 5.0, \\ & 0 < K_d \le 10 \end{array}\right\} \tag{36}$$

$$G_c(s)|_{PID\_CS} = 5.02 + \frac{0.89}{s} + 0.99s \tag{37}$$

5.3. **Robust PIDA controller designed by CS.** Referring to Figure 7, the CS-based robust PIDA design framework for the interaction 3-tank liquid-level system can be conducted. Model additive uncertainty $\Delta(s) = \pm 10\%$ of each lumped parameter of the nominal plant model is assumed for the nominal plant model $G_p(s)$ in (28). Thus, the plant model $\tilde{G}_p(s)$ in (27) can be rewritten as stated in (38). The objective function $f$ in (25) is conducted.

$$\tilde{G}_p(s) = \frac{1}{(0.5 \pm \Delta)s^3 + (3 \pm \Delta)s^2 + (4.5 \pm \Delta)s + 1} \tag{38}$$

$$\left.\begin{array}{ll} \text{Subject to} & t_r \le 2.5 \text{ sec.}, \\ & M_p \le 20.0\%, \\ & t_s \le 15.0 \text{ sec.}, \\ & E_{ss} \le 0.01\%, \\ & 0 < K_p \le 30, \\ & 0 < K_i \le 5.0, \\ & 0 < K_d \le 10, \\ & 0 < K_a < 5.0, \\ & [G_p(s) - \Delta(s)] \le G_p(s) \le [G_p(s) + \Delta(s)] \end{array}\right\} \tag{39}$$

$$G_c(s)|_{PIDA\_CS} = 25.03 + \frac{3.04}{s} + 9.98s + 3.01s^2 \tag{40}$$

Like a case of the CS-based PID controller design, the CS algorithm was coded by MATLAB version 2018b (License No.#40637337) run on Intel(R) Core(TM) i5-3470 CPU@3.60 GHz, 4.0 GB-RAM. Number of cuckoos $n = 40$ and fraction $p_a = 0.2$ are set according to recommendations of Yang and Deb [3,4]. This searching parameters setting is sufficient for most optimization problems. Search spaces and constraint functions are then performed as shown in (39). The maximum generation Max_Gen = 100 is then set as the TC. 50 trials are conducted to find the best solution (optimal robust PIDA controller for the interaction 3-tank liquid-level system). Once the search process stopped, the CS

can successfully provide the optimal parameters of the PIDA controller of the interaction 3-tank liquid-level system as expressed in (40).

For comparison of the system responses, the step-input responses and the step-disturbance responses of the interaction 3-tank liquid-level system without, with the PID controllers designed by ZN in (34), by the CS in (37) and the robust PIDA controller designed by the CS in (40) are plotted in Figure 8 and Figure 9, respectively. Those system responses are summarized in Table 2, where $t_{reg}$ is the regulating time, $M_{p\_reg}$ is the percent maximum overshoot from load disturbance regulation and $E_{ss\_reg}$ is the steady-state error from load disturbance regulation.

From Figure 8 and Figure 9 as well as Table 2, it can be observed that the interaction 3-tank liquid-level controlled system with the robust PIDA controller designed by the CS can provide more satisfactory responses with faster and smoother than with the PID controllers designed by ZN and CS, significantly.

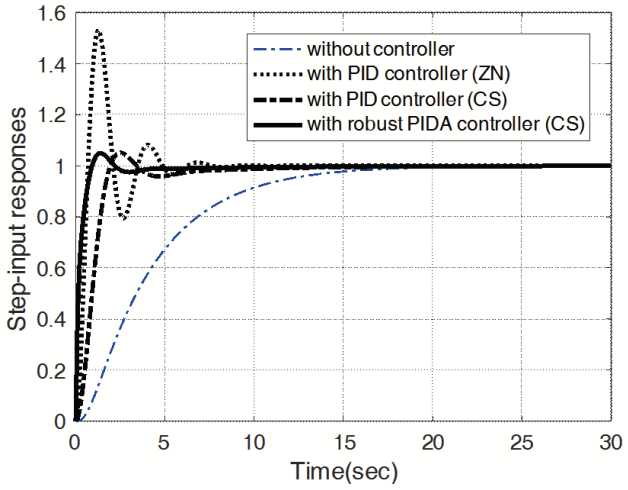


FIGURE 8. Step-input responses of the 3-tank liquid-level system without and with PID controllers designed by ZN and CS and with PIDA controller designed by the CS

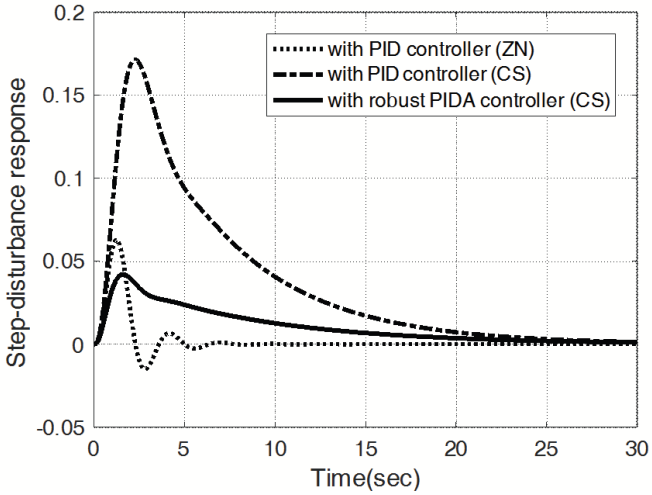


FIGURE 9. Step-disturbance responses of the 3-tank liquid-level system with PID controllers designed by ZN and CS and with PIDA controller designed by the CS

TABLE 2. Responses of the interaction 3-tank liquid-level system without, with PID and robust PIDA controllers

| Controllers | System responses | | | | | | |
|---|---|---|---|---|---|---|---|
| | Step-input responses | | | | Step-disturbance responses | | |
| | $t_r$ (s) | $M_p$ (%) | $t_s$ (s) | $E_{ss}$ (%) | $M_{p\_reg}$ (%) | $t_{reg}$ (s) | $E_{ss\_reg}$ (%) |
| Without controller | 8.54 | 0.00 | 15.41 | 0.00 | – | – | – |
| PID (by ZN) | 0.68 | 53.13 | 5.85 | 0.00 | 6.28 | 2.42 | 0.00 |
| PID (by CS) | 1.92 | 6.42 | 8.36 | 0.00 | 17.14 | 15.37 | 0.00 |
| Robust PIDA (by CS) | 0.91 | 4.95 | 3.47 | 0.00 | 4.20 | 7.46 | 0.00 |

5.4. **Robust stability and robust performance investigations.** In order to investigate robust stability and robust performance of the interaction 3-tank liquid-level controlled systems, the additive model uncertainty due to 500 variations of each lumped parameter of the nominal plant model in (38) within $\Delta(s) = \pm 10\%$ is randomly generated to simulate the perturbation due to aging and environmental effects. The step responses of the interaction 3-tank liquid-level system with the PID controller designed by the ZN in (34) are plotted in Figure 10. It was found that all system responses with the PID controller in (34) do not satisfy to inequality constraint functions in (39). This means that the system with the PID controller designed by the ZN is non-robust performance. Once their poles and zeros are plotted in Figure 11, it can be observed that all poles are located on the left-hand side (LHS) of the complex plain. This implies that the interaction 3-tank liquid-level system with the PID controller designed by the ZN is robust stability.

By using the PID controller designed by the CS in (37) with model uncertainty, 500 variations of each lumped parameter of the nominal plant model in (38) within $\Delta(s) = \pm 10\%$ are randomly generated to simulate the perturbation. The step responses of the interaction 3-tank liquid-level controlled system with the PID controller designed by the CS are depicted in Figure 12. It was found that all system responses with the PID controller in (37) satisfy to inequality constraint functions in (39). This means that the system with the PID controller designed by the CS is robust performance. Regarding

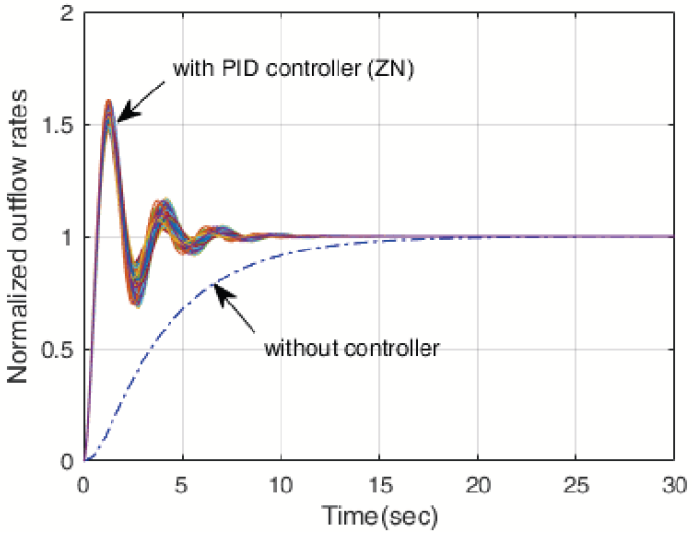


FIGURE 10. Step-input responses of the 3-tank liquid-level system controlled by PID controller designed by ZN with model uncertainty

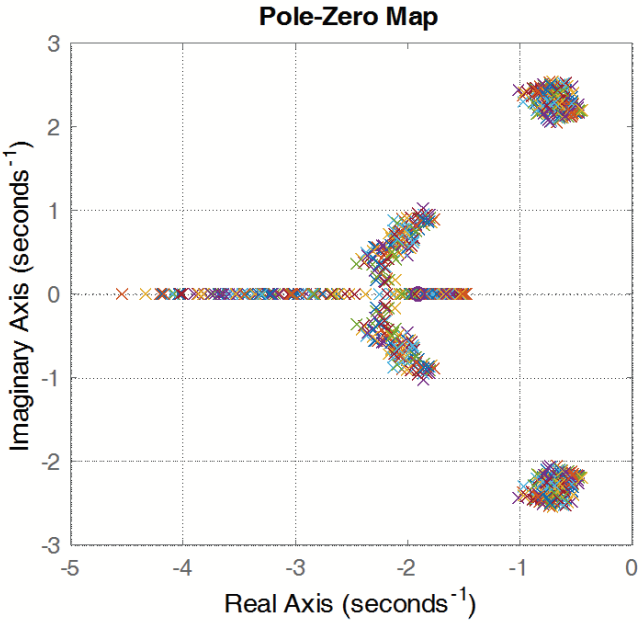


FIGURE 11. Pole-zero plots of the 3-tank liquid-level system controlled by PID controller designed by ZN with model uncertainty

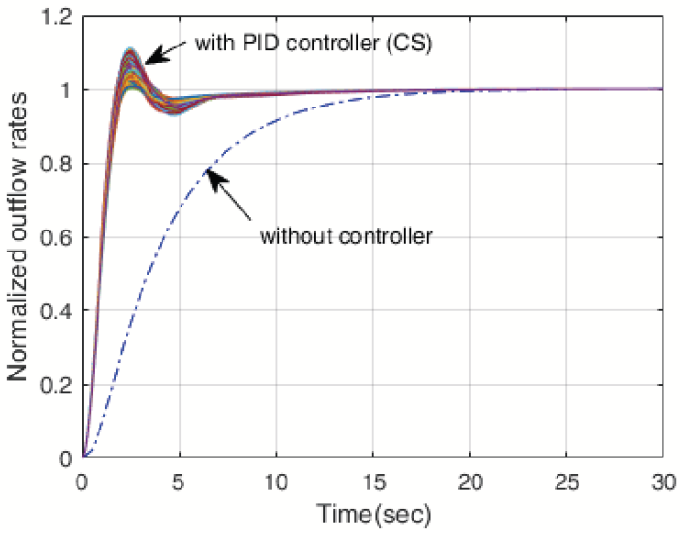


FIGURE 12. Step-input responses of the 3-tank liquid-level system controlled by PID controller designed by CS with model uncertainty

to robust control theory [28-30], if the system is robust performance, the system is also robust stability. This can be proved by the pole-zero plots in Figure 13.

Finally, by using the robust PIDA controller designed by the CS in (40) with model uncertainty, 500 variations of each lumped parameter of the nominal plant model in (38) within $\Delta(s) = \pm 10\%$ are randomly generated to simulate the perturbation. The step responses of the interaction 3-tank liquid-level controlled system with the robust PIDA controller are depicted in Figure 14. It was found that all system responses with the robust PIDA controller in (40) strongly satisfy to inequality constraint functions in (39). The system with the robust PIDA controller designed by the CS is robust performance, while robust stability can be proved by the pole-zero plots in Figure 15.

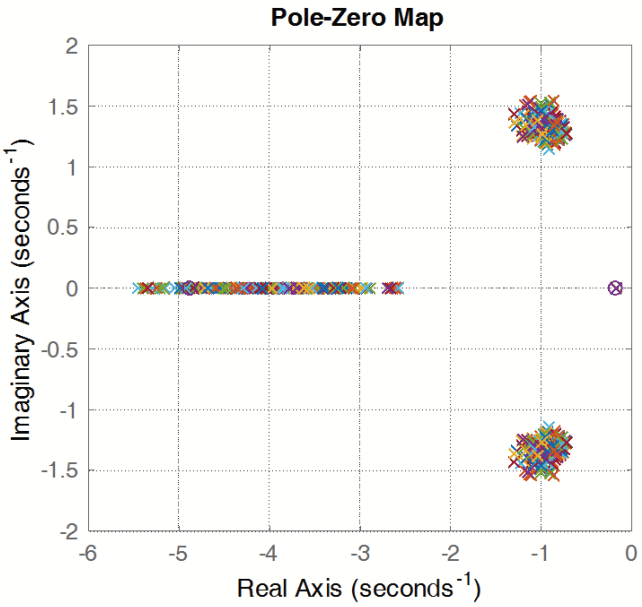


FIGURE 13. Pole-zero plots of the 3-tank liquid-level system controlled by PID controller designed by CS with model uncertainty

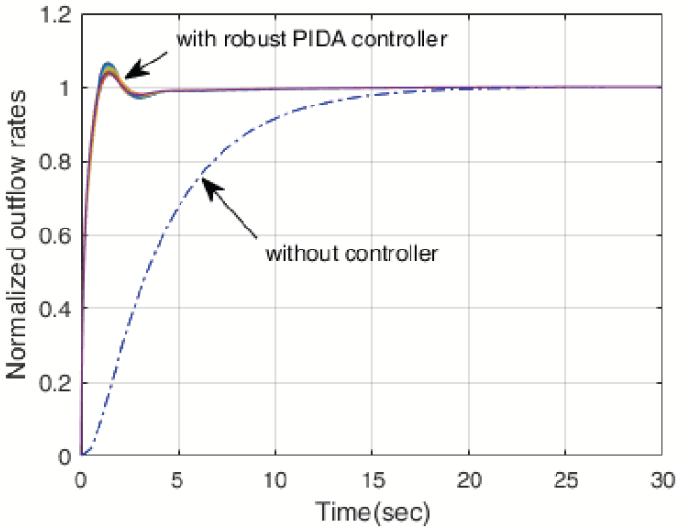


FIGURE 14. Step-input responses of the 3-tank liquid-level system controlled by robust PIDA controller designed by CS with model uncertainty

By comparison among Figure 10, Figure 12 and Figure 14 when model uncertainty is presented within $\Delta(s) = \pm 10\%$, the deviation of the step responses of the system with PID designed by the ZN is the largest. Deviation of the step responses of the system with PID designed by the CS is greater than those with the robust PIDA controller designed by the CS. Once considering the differences among Figure 11, Figure 13 and Figure 15, it can be observed that the deviation of pole-zero locations of the system with PID controller designed by the ZN is the largest. Deviation of pole-zero locations of the system with PID controller designed by the CS is greater than those with robust PIDA controller designed by the CS. This can be concluded that the robust PIDA controller designed by the CS provides the very satisfactory responses of the interaction 3-tank liquid-level

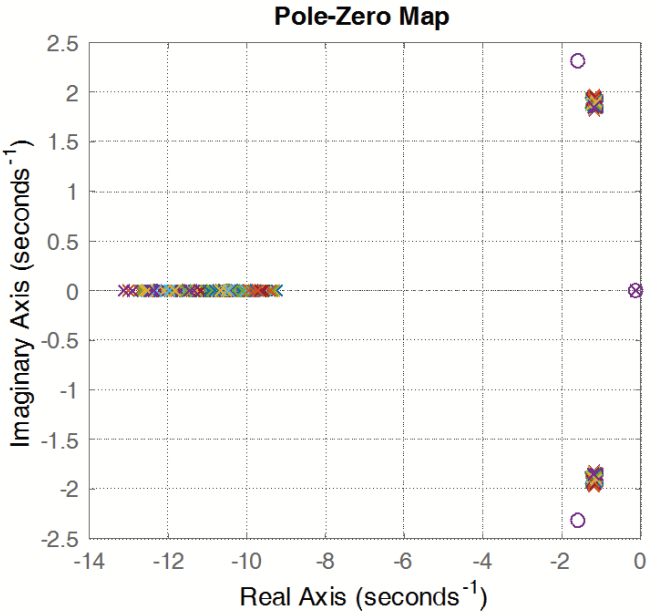


FIGURE 15. Pole-zero plots of the 3-tank liquid-level system controlled by robust PIDA controller designed by CS with model uncertainty

controlled system with model uncertainty superior to PID controllers designed by ZN and CS, respectively.

6. **Conclusions.** Application of the CS to robust PIDA controller design for the interaction 3-tank liquid-level system has been proposed. The CS algorithm has been briefly reviewed and the concepts of robust control system have been briefly described. The robust stability and robust performance have been set as the inequality constraints of the robust PIDA controller design approach by the CS. As results, the 3-tank liquid-level controlled system with the PID controller designed by ZN provided very fast step-input and step-disturbance responses with very high overshoot. The 3-tank liquid-level controlled system with the PID controller designed by CS yielded slower step-input and step-disturbance responses with lower overshoot, while those with the robust PIDA controller designed by CS provided very fast step-input and step-disturbance responses with lower overshoot. For stability analysis, it was found that the system with the PID controller designed by the ZN is robust stability, but non-robust performance. In contrast, the systems with the PID and the robust PIDA controllers designed by the CS are robust performance and robust stability. The robust PIDA controller designed by the CS provided the very satisfactory responses of the interaction 3-tank liquid-level controlled system with model uncertainty better than the PID controllers designed by ZN and CS. For the future research, the metaheuristics-based control design optimization framework will be extended to other real-world control engineering problems including linear and nonlinear systems.

## REFERENCES

[1] E. G. Talbi, *Metaheuristics: Form Design to Implementation*, John Wiley & Sons, Hoboken, 2009.
[2] X. S. Yang, *Engineering Optimization: An Introduction with Metaheuristic Applications*, John Wiley & Sons, 2010.
[3] X. S. Yang and S. Deb, Cuckoo search via Lévy flights, *Proc. of the World Congress on Nature & Biologically Inspired Computing (NaBIC 2009)*, pp.210-214, 2009.

[4] X. S. Yang, Cuckoo search and firefly algorithm: Overview and analysis, in *Cuckoo Search and Firefly Algorithm: Theory and Applications*, X.-S. Yang (ed.), Cham, Springer, 2014.
[5] B. Ernst, M. Bloh, J. R. Seume and A. G. González, Implementation of the cuckoo search algorithm to optimize the design of wind turbine rotor blades, *Proc. of the European Wind Energy Association (EWEA 2012)*, 2012.
[6] M. Khodier, Optimisation of antenna arrays using the cuckoo search algorithm, *IET Microwaves, Antennas & Propagation*, vol.7, no.6, pp.458-464, 2013.
[7] S. Rangasamy and P. Manickam, Stability analysis of multimachine thermal power systems using nature inspired modified cuckoo search algorithm, *Turkish Journal of Electrical Engineering & Computer Sciences*, DOI: 10.3906/elk-1212-39, 2013.
[8] A. Ouaarab, B. Ahiod and X. S. Yang, Discrete cuckoo search algorithm for the travelling salesman problem, *Neural Computing and Applications*, pp.1-11, 2013.
[9] A. H. Gandomi, X. S. Yang and A. H. Alavi, Cuckoo search algorithm: A metaheuristic approach to solve structural optimization problems, *Engineering with Computers*, vol.29, no.1, pp.17-35, 2013.
[10] M. Dhivya and M. Sundarambal, Cuckoo search for data gathering in wireless sensor networks, *International Journal of Mobile Communications*, vol.9, no.6, pp.642-656, 2011.
[11] M. K. Marichelvam, An improved hybrid cuckoo search (IHCS) metaheuristics algorithm for permutation flow shop scheduling problems, *International Journal of Bio-Inspired Computation*, vol.4, no.4, pp.200-205, 2012.
[12] S. Hanoun, S. Nahavandi, D. Creighton and H. Kull, Solving a multiobjective job shop scheduling problem using pareto archived cuckoo search, *Proc. of the 17th IEEE Conference on Emerging Technologies & Factory Automation (ETFA)*, pp.1-8, 2012.
[13] S. Hlungnamthip and D. Puangdownreong, Model order reduction of linear time-invariant dynamic systems via cuckoo search, *KMUTT Research & Development Journal*, vol.40, no.2, pp.237-253, 2017.
[14] D. Puangdownreong, A. Nawikavatan and C. Thammarat, Optimal design of I-PD controller for DC motor speed control system by cuckoo search, *Procedia Computer Science*, vol.86, pp.83-86, 2016.
[15] I. Fister, Jr., X. S. Yang, D. Fister and I. Fister, Cuckoo search: A brief literature review, in *Cuckoo Search and Firey Algorithm: Theory and Applications*, X.-S. Yang (ed.), Cham, Springer, 2014.
[16] B. G. Liptak, *Instrumentation Engineer's Handbook' Process Control*, CRC Press, 1995.
[17] A. Dwyer, *Handbook of PI and PID Controller Tuning Rules*, Imperial College, 2009.
[18] S. Jung and R. C. Dorf, Analytic PIDA controller design technique for a third order system, *Proc. of the 35th IEEE Conference on Decision and Control*, Kobe, pp.2513-2518, 1996.
[19] S. Sornmuang and S. Sujitjorn, GA-based PIDA control design optimization with an application to AC motor speed control, *International Journal of Mathematics and Computers in Simulation*, vol.4, no.3, pp.67-80, 2010.
[20] D. Puangdownreong and S. Suwannarongsri, Torsional resonance suppression via PIDA controller designed by the particle swarm optimization, *Proc. of the ECTI-CON International Conference*, pp.673-676, 2008.
[21] D. Puangdownreong, Application of current search to optimum PIDA controller design, *Intelligent Control and Automation*, vol.3, no.4, pp.303-312, 2012.
[22] D. Puangdownreong, S. Sumpunsri, M. Sukchum, C. Thammarat, S. Hlangnamthip and A. Nawikavatan, FA-based optimal PIDA controller design for AVR system, *Proc. of the iEECON2018 International Conference*, pp.548-551, 2018.
[23] C. Thammarat, K. Lurang, D. Puangdownreong, S. Suwammarongsri, S. Hlangnamthip and A. Nawikavatan, Application of bat-inspired algorithm to optimal PIDA controller design for liquid-level system, *Proc. of the iEECON2018 International Conference*, pp.556-559, 2018.
[24] K. Lurang, C. Thammarat, S. Hlangnamthip and D. Puangdownreong, Optimal design of two-degree-of-freedom PIDA controllers for liquid-level system by bat-inspired algorithm, *International Journal of Circuits, Systems and Signal Processing*, vol.13, pp.34-39, 2019.
[25] T. Niyomsat and D. Puangdownreong, Optimal PIDA load frequency controller design for power systems via flower pollination algorithm, *WSEAS Trans. Power Systems*, vol.14, pp.1-7, 2019.
[26] N. Pringsakul, D. Puangdownreong, C. Thammarat and S. Hlangnamthip, Obtaining optimal PIDA controller for temperature control of electric furnace system via flower pollination algorithm, *WSEAS Trans. Systems and Control*, vol.14, pp.1-7, 2019.
[27] A. Nawikavatan, T. Jitwang, C. Thammarat and D. Puangdownreong, Application of cuckoo search to optimal PIDA controller design for three-tank liquid-level control system, *Proc. of the 2018 International Conference on Engineering and Natural Science (ICENS 2018)*, pp.51-59, 2018.

[28] K-Z. Liu and Y. Yao, *Robust Control Theory and Applications*, John Wiley & Sons, 2016.
[29] K. Zhou, J. C. Doyle and K. Glover, *Robust and Optimal Control*, Prentice Hall, 1996.
[30] K. Zhou and J. C. Doyle, *Essentials of Robust Control*, Prentice Hall, 1998.
[31] P. Konghuayrob, S. Kaitwanidvilai and H. Aoyama, Hybrid adaptive notch filter and fixed-structure PID $H_\infty$ robust loop shaping control based PSO for hard disk drive servo actuator, *International Journal of Innovative Computing, Information and Control*, vol.15, no.1, pp.1-20, 2019.
[32] P. Konghuayrob and S. Kaitwanidvilai, Specified order – $H_\infty$ loop shaping control for hard disk drive servo using PSO, *International Journal of Innovative Computing, Information and Control*, vol.12, no.4, pp.1241-1255, 2016.
[33] Y. C. Fung, *Biomechanics – Motion, Flow, Stress and Growth*, New York (USA), Springer-Verlag, 1990.
[34] J. Arulvadivu, N. Divya and S. Manoharan, Integrated PID based intelligent control for three-tank system, *ARPN Journal of Engineering and Applied Sciences*, vol.10, no.9, pp.4013-4017, 2015.
[35] J. G. Ziegler and N. B. Nichols, Optimum settings for automatic controllers, *Trans. ASME*, vol.64, pp.759-768, 1942.
[36] J. G. Ziegler and N. B. Nichols, Process lags in automatic control circuits, *Trans. ASME*, vol.65, pp.433-444, 1943.